Excitations in photonic crystals infiltrated with polarizable media

A. Yu. Sivachenko, M. E. Raikh, and Z. V. Vardeny
Department of Physics, University of Utah, Salt Lake City, Utah 84112
(Received 3 November 2000; published 8 June 2001)

Light propagation in a photonic crystal with incomplete band gap, infiltrated with polarizable molecules is considered. We demonstrate that the interplay between the spatial dispersion caused by Bragg diffraction and polaritonic frequency dispersion gives rise to alternative propagating excitations, or photonic-crystal-polaritons (PCP), with intragap frequencies. We derive the PCP dispersion relation and show that it is governed by two parameters, namely, the strength of light-matter interaction and detuning between the Bragg frequency and that of the infiltrated molecules. We also study defect-induced states when the photonic band gap is divided into two subgaps by the PCP branches and find that each defect creates *two* intragap localized states inside *each* subgap.

DOI: 10.1103/PhysRevA.64.013809 PACS number(s): 42.50.Ct, 71.36.+c, 42.70.Qs

I. INTRODUCTION

Photonic crystals and, in particular, photonic band-gap (PBG) materials [1,2], have recently attracted much attention [3,4] due to their rich physics and possible applications. In these systems the dielectric function is periodically modulated and, as a result, their optical properties are dominated by light diffraction effects. When Bragg diffraction conditions are met then light scattering is very strong, so that within certain frequency intervals near the resonances light propagation is inhibited.

Since the subject of photonic crystals was introduced [1,2], one of the main goals of photonic band-structure calculations has been to engineer structures with a *complete* band gap, i.e., with no propagating solutions of Maxwell's equations within a certain *forbidden gap*. The pursuit of this goal has generated a stream of studies that are too numerous to be cited here; early works are reviewed in Refs. [3,4]. Here we only mention that a complete band gap in two dimensions (2D) was theoretically predicted [5,6] and experimentally demonstrated [5] for an array of dielectric rods. In the quest for a structure having a complete PBG in three dimensions (3D), the diamond lattice was shown [7] to be more promising than a simple face-centered-cubic (fcc) lattice [7,8].

The frequency gap in the photonic spectrum sets a stage for a number of physical effects. The prime effect, namely the inhibition of spontaneous emission for an emitter with transition frequency within the gap, was already suggested in the pioneering works [1,9,10]. Furthermore, since light cannot leave the emitting atom, a coupled atom-field in-gap state is formed, in which the atomic level is ''dressed'' by its own exponentially localized radiation field [9,11]. It was also demonstrated that although a single photon cannot propagate inside the gap, nevertheless, a nonlinear medium embedded inside the photonic crystal gives rise to multiphoton bound states [12], or gap solitons [13] that result in self-induced transparency. Yet another consequence of PBG is the modification of cooperative emission with frequency close to the band edge. In particular, the PBG was shown to change the rate of superradiant emission from an ensemble of emitters [10,14]. Lastly, PBG structures facilitate strong Anderson localization of photons [15] because the sharp density of states within the gap spectral range necessitates a reinterpretation of the Ioffe-Regel criterion [2].

PBG structures with a defect constitute a separate area of study initiated by the classical works in Refs. [5,16]. These structures are important since the defects cause localized intragap states. For these states, the PBG sample acts as a resonator with a very high quality factor. This property was recently used for designing a low-threshold PBG defect-mode laser [17].

Another class of materials with a forbidden gap for light propagation is spatially homogeneous, but frequency-dispersive media. The energy gap in these systems has a polaritonic origin, i.e., it is formed due to the interaction of light with the medium polarization [18]. This energy gap can be viewed as the result of anticrossing between the photonic and excitonic dispersion relation branches. Some nontrivial manifestations of the polaritonic gap were recently explored in Refs. [19,20]. In these papers a general model of two-level systems interacting with elementary electromagnetic excitations with a gap in the spectrum was solved by means of the Bethe ansatz technique. Within this model a very rich excitation spectrum was found [19,20], consisting of ordinary solitons, single-particle impurity bound states, and massive pairs of confined gap excitations and their bound complexes — dissipationless quantum gap solitons.

Most of the available photonic crystals nowadays, however, have *incomplete* PBGs; this means that light propagation is forbidden only along certain directions inside the crystal. A prominent example is opals, representing self-assembled monodispersed silica balls [21] arranged in a fcc type lattice. Although opals have only an incomplete PBG, the voids between the balls can be infiltrated by various media, which brings about nontrivial physics. In particular, the medium may contain polarizable molecules. Infiltrated opal with polarizable molecules combines therefore polaritonic and Bragg-diffractive properties. Obviously, both effects coexist independently when the Bragg ($\omega=\omega_B$) and polaritonic ($\omega=\omega_T$) resonances are well separated in frequency. A completely different situation occurs when $\omega_B \approx \omega_T$. This may be easily achieved in infiltrated opals that gives rise to a

 ©2001 The American Physical Society

peculiar *interplay* between various frequency dispersions. This interplay is the subject of the present paper.

Our most important finding pertains to the case when the polaritonic gap of the polarized molecules infiltrating the opal lies within the opal PBG. We demonstrate that such an overlap gives rise to massive *propagating* excitations having frequencies inside the Bragg gap, which we refer to as photonic-crystal-polaritons (PCPs). In other words, the Bragg gap *splits* into two subgaps, so that the PCP branches are isolated from the rest of the spectrum. We found that the PCP dispersion relation is very sensitive to the frequency detuning between ω_B and ω_T and to the relative width of the polaritonic gap (or, alternatively Rabi frequency) and the Bragg gap.

The principal assumption we adopt here is that the Bragg gap, $\Delta\omega_B$, is narrow compared to ω_B; this is actually the case in opals. The small value of $\Delta\omega_B/\omega_B \ll 1$ enables us then to obtain analytical results. In addition, we also study the phase slip related intragap defect states for $\omega_B \approx \omega_T$. In the absence of polaritonic effect, the underlying physics of the defect-induced intragap states was already discussed in the original PBG paper [1]. An analogy was drawn between a defect state and a localized mode in a distributed feedback resonator, which originates from a phase slip. We extend this picture to incorporate the polarizable medium and show that when the Bragg gap splits into two subgaps, then an existing phase slip gives rise to *two* localized states with frequencies within *each* of the subgaps.

Our paper is organized as follows: In order to introduce the notations, we separately review in Sec. II the derivation of the PBG and polaritonic spectra using the second quantization representation. In Sec. III we consider the combined Hamiltonian in the second quantization representation and diagonalize it by a unitary transformation. This yields the dispersion relations for the two excitations outside the gap, or Bloch-like waves, and the two intragap branches, or PCP excitations. The properties of these excitations are analyzed in Sec. IV. We use them in Sec. V to determine the intragap frequencies of the defect-induced localized states. Concluding remarks are presented in Sec. VI.

II. SECOND QUANTIZED PBG AND POLARITONIC HAMILTONIANS

The Hamiltonian $\mathcal{H}$ of the system under study is the sum of three terms

$$\mathcal{H}=\mathcal{H}_{\rm ph}+\mathcal{H}_m+\mathcal{H}_{m\text{-ph}}. \tag{1}$$

The first term $\mathcal{H}_{\rm ph}$ describes the photons in a photonic crystal. The second term $\mathcal{H}_m$ is the Hamiltonian of the polarizable medium; $\mathcal{H}_{m\text{-ph}}$ describes the photon-medium coupling. In this section we review two limiting cases: (i) no polarizable medium ($\mathcal{H}_m \equiv 0$), and (ii) no modulation of the dielectric constant.

A. Incomplete PBG

The general form of the Hamiltonian $\mathcal{H}_{ph}$ is

$$\mathcal{H}_{\rm ph}=\frac{1}{8\pi}\int d\boldsymbol{r}[\varepsilon(\boldsymbol{r})\boldsymbol{E}^2+\boldsymbol{H}^2], \tag{2}$$

where $\boldsymbol{E}$ and $\boldsymbol{H}$ are, respectively, the electric and magnetic fields. For a constant dielectric function, $\varepsilon(\boldsymbol{r})\equiv\varepsilon_0$, the second quantized form [22] of the Hamiltonian (2) reduces to a sum over oscillators representing plane waves with frequencies $\omega_k = ck/\sqrt{\varepsilon_0}$, where k is the wave vector. Modulation of $\varepsilon(\boldsymbol{r})$ causes light diffraction, so that the plane-wave solutions are no longer the correct eigenfunctions of the Hamiltonian (2). Below we consider a photonic crystal with an incomplete PBG along the z axis. A particular example is opals, which are self-assembled photonic crystals made of silica balls. The gradient of the refractive index is small enough [21] so that the width of the incomplete PBG is relatively small. Thus, the situation can be adequately approximated by a one-dimensional modulation of $\varepsilon(\boldsymbol{r})$ along the z direction, with only a single harmonics taken into account:

$$\varepsilon(z)=\varepsilon_0+\delta\varepsilon\cos(\sigma z+\phi). \tag{3}$$

Here $\delta\varepsilon$ ($\ll\varepsilon_0$) is the modulation amplitude, $\sigma=2\pi/d$, where d is the modulation period, and ϕ is the dielectric modulation phase. We assume for simplicity that the electromagnetic field propagates along the z direction and is homogeneous in the xy plane. In this case light polarization is irrelevant. Generalization to arbitrary propagation direction is straightforward. The Fourier components of $\varepsilon(z)$ in Eq. (3) couple the original photon oscillators with momenta k and $k\pm\sigma$. These coupled oscillators form an infinite series that is constructed by successive addition (subtraction) of σ. However, if $\delta\varepsilon \ll \varepsilon_0$ and the wave-vector domain is restricted to the vicinity of the first Bragg resonance at $k\approx\sigma/2$, then the Hamiltonian (2) can be truncated. In this case, only the coupling to the near-resonance backscattered photons with momenta $(\sigma-k)\approx\sigma/2$ must be retained, so that the Hamiltonian (2) takes the form

$$\mathcal{H}_{ph}=\sum_q \{\omega(q)\hat{a}^+_{\rightarrow}(q)\hat{a}_{\rightarrow}(q)+\omega(-q)\hat{a}^+_{\leftarrow}(-q)\hat{a}_{\leftarrow}(-q) + \Omega_B[e^{i\phi}\hat{a}^+_{\rightarrow}(q)\hat{a}_{\leftarrow}(-q)+e^{-i\phi}\hat{a}^+_{\leftarrow}(-q)\hat{a}_{\rightarrow}(q)]\}. \tag{4}$$

Here, we introduced the notations $q=k-\sigma/2$, $\hat{a}_{\rightarrow}(q)=\hat{a}_k$ and $\hat{a}_{\leftarrow}(-q)=\hat{a}_{k-\sigma}$ for $k\approx\sigma/2$, where $\hat{a}_k$ is the usual photon annihilation operator. In the notations introduced in Eq. (4), the frequencies of the photonic branches are given by

$$\omega(q)=\frac{c(q+\sigma/2)}{\sqrt{\varepsilon_0}}=\omega_B\left(1+\frac{2q}{\sigma}\right), \tag{5}$$

where $\omega_B=c\sigma/(2\sqrt{\varepsilon_0})$ is the Bragg frequency. We define the coupling constant, Ω_B, as the half-width of the Bragg gap, i.e., $\Omega_B=\frac{1}{2}\Delta\omega_B$. It can be shown that Ω_B is related to

the amplitude of the dielectric function modulation: $\Omega_B = \omega_B \delta\varepsilon/(2\varepsilon_0)$. The summation in Eq. (4) is performed over the k domain $|q| \ll \sigma/2$.

It is straightforward to diagonalize the Hamiltonian in Eq. (4) with the use of the following unitary transformation:

$$\hat{a}_{\rightarrow}(q) = \cos\theta \hat{\beta}_1(q) + \sin\theta e^{i\phi}\hat{\beta}_2(q),$$

$$\hat{a}_{\leftarrow}(-q) = -\sin\theta e^{-i\phi}\hat{\beta}_1(q) + \cos\theta\hat{\beta}_2(q), \tag{6}$$

where

$$\cos 2\theta = \frac{\omega(q) - \omega(-q)}{\sqrt{[\omega(q) - \omega(-q)]^2 + 4\Omega_B^2}}. \tag{7}$$

The new operators $\hat{B}_1$ and $\hat{B}_2$ describe the creation (annihilation) of pairs of Bloch waves that consist of forward and backscattered photons near the Bragg frequency. The diagonalized Hamiltonian (4) takes the form

$$\mathcal{H}_{ph} = \sum_q \omega_B^{(1)}(q)\hat{\beta}_1^+(q)\hat{\beta}_1(q) + \omega_B^{(2)}(q)\hat{\beta}_2^+(q)\hat{\beta}_2(q), \tag{8}$$

where the dispersion relations of the two photonic branches are given by

$$\begin{aligned}\omega_B^{(1,2)}(q) &= \frac{1}{2}[\omega(q) + \omega(-q) \\ &\quad \pm \sqrt{(\omega(q) - \omega(-q))^2 + 4\Omega_B^2}] \\ &= \omega_B \pm \sqrt{\left(\frac{2\omega_B}{\sigma}\right)^2 q^2 + \Omega_B^2}.\end{aligned} \tag{9}$$

As mentioned above, the width of the PBG from Eq. (9) is $2\Omega_B$.

B. Polarizable medium

The Hamiltonians $\mathcal{H}_m$ of the polarizable medium and $\mathcal{H}_{m\text{-ph}}$ of light-polarization interaction in Eq. (1) can be written in the second quantization form as

$$\mathcal{H}_m + \mathcal{H}_{m\text{-ph}} = \omega_T \sum_k \hat{b}_k^+ \hat{b}_k + \Omega_P \sum_k [\hat{b}_k^+ \hat{a}_k + \hat{a}_k^+ \hat{b}_k], \tag{10}$$

where $\hat{b}$ is the annihilation operator of the medium excitations (e.g., excitons or optical phonons), which we assume here to be dispersionless having frequency ω_T; Ω_P denotes the light-medium coupling strength that is proportional to the Rabi frequency. In the absence of the Bragg scattering term ($\Omega_B = 0$), the complete Hamiltonian (1) reduces to the conventional polaritonic Hamiltonian $\mathcal{H}_{pol}$, given by

$$\mathcal{H}_{pol} = \sum_k \omega_k \hat{a}_k^+ \hat{a}_k + \omega_T \sum_k \hat{b}_k^+ \hat{b}_k + \Omega_P \sum_k [\hat{b}_k^+ \hat{a}_k + \hat{a}_k^+ \hat{b}_k], \tag{11}$$

with eigenstates representing the mixture of light and medium excitations

$$\hat{a}_k = \cos\psi\hat{\pi}_1(k) + \sin\psi\hat{\pi}_2(k),$$

$$\hat{b}_k = -\sin\psi\hat{\pi}_1(k) + \cos\psi\hat{\pi}_2(k), \tag{12}$$

where

$$\cos 2\psi = \frac{\omega_k - \omega_T}{\sqrt{(\omega_k - \omega_T)^2 + 4\Omega_P^2}} \quad (\omega_k = ck/\sqrt{\varepsilon_0}). \tag{13}$$

With the new operators $\hat{\pi}_1$ and $\hat{\pi}_2$, the Hamiltonian (11) is diagonalized:

$$\mathcal{H}_{pol} = \sum_k \omega_P^{(1)}(k)\hat{\pi}_1^+(k)\hat{\pi}_1(k) + \sum_k \omega_P^{(2)}(k)\hat{\pi}_2^+(k)\hat{\pi}_2(k), \tag{14}$$

where the frequencies of the polaritonic branches are given by

$$\omega_P^{(1,2)}(k) = \frac{1}{2}[\omega_k + \omega_T \pm \sqrt{(\omega_k - \omega_T)^2 + 4\Omega_P^2}]. \tag{15}$$

The Rabi splitting at resonance, i.e., at $\omega_k = \omega_T$ is $2\Omega_P$. Equation (15) allows one to express the phenomenological parameter Ω_P through the observables. Namely, $\Omega_P = \sqrt{\omega_T \omega_{LT}/2}$, where $\omega_{LT} \ll \omega_T$ is the transverse-longitudinal splitting.

We note that the above description is valid only for wave numbers k in the vicinity of ''crossing'' of the excitation branches, where $\omega_k \simeq \omega_T$. It does not capture, however, the correct behavior [18] of the polaritonic branches for $k \to 0$. In this limit an additional term of the type $a_k b_{-k}$ + c.c. should be taken into account in Eq. (11). Under the same condition, $\omega_k \simeq \omega_T$, the dispersion relation Eq. (15) can also be derived from the wave equation with the frequency-dependent dielectric function.

III. DIAGONALIZATION OF THE FULL HAMILTONIAN

Now let us consider the full Hamiltonian (1) with both Bragg scattering and light-medium interaction included,

$$\begin{aligned}\mathcal{H} &= \sum_q [\omega(q)\hat{a}_{\rightarrow}^+(q)\hat{a}_{\rightarrow}(q) + \omega(-q)\hat{a}_{\leftarrow}^+(-q)\hat{a}_{\leftarrow}(-q)] \\ &\quad + \Omega_B \sum_q [e^{i\phi}\hat{a}_{\rightarrow}^+(q)\hat{a}_{\leftarrow}(-q) + e^{-i\phi}\hat{a}_{\leftarrow}^+(-q)\hat{a}_{\rightarrow}(q)] \\ &\quad + \omega_T \sum_q [\hat{b}_{\rightarrow}^+(q)\hat{b}_{\rightarrow}(q) + \hat{b}_{\leftarrow}^+(-q)\hat{b}_{\leftarrow}(-q)] \\ &\quad + \Omega_P \sum_q [\hat{b}_{\rightarrow}^+(q)\hat{a}_{\rightarrow}(q) + \hat{a}_{\rightarrow}^+(q)\hat{b}_{\rightarrow}(q) \\ &\quad + \hat{b}_{\leftarrow}^+(-q)\hat{a}_{\leftarrow}(-q) + \hat{a}_{\leftarrow}^+(-q)\hat{b}_{\leftarrow}(-q)],\end{aligned} \tag{16}$$

where we have again truncated the ''Bragg'' Hamiltonian in Eq. (1) by including only near-resonance terms. If a column of operators $\hat{c}=\{\hat{a}_{\rightarrow}(q),\hat{a}_{\leftarrow}(-q),\hat{b}_{\rightarrow}(q),\hat{b}_{\leftarrow}(-q)\}$ is introduced, then the Hamiltonian (16) can be formally rewritten in a matrix form $\mathcal{H}=\hat{c}^{+}H\hat{c}$, where

$$H=\begin{pmatrix} \omega(q) & \Omega_B e^{i\phi} & \Omega_P & 0 \\ \Omega_B e^{-i\phi} & \omega(-q) & 0 & \Omega_P \\ \Omega_P & 0 & \omega_T & 0 \\ 0 & \Omega_P & 0 & \omega_T \end{pmatrix}. \tag{17}$$

The four H eigenvalues yield the dispersion relations of the *four* excitation branches, whereas the eigenvectors determine the unitary transformation diagonalizing $\mathcal{H}$.

The characteristic equation for the eigenvalues ω of the matrix H reads

$$\left[(\omega(q)-\omega)(\omega(-q)-\omega)-\Omega_B^2 - \left(\frac{\omega(q)+\omega(-q)-2\omega}{\omega_T-\omega}\right)\Omega_P^2\right](\omega_T-\omega)^2+\Omega_P^4=0. \tag{18}$$

If the light-matter coupling is absent, i.e., $\Omega_P=0$, then the roots of Eq. (18) reduce to two pure medium excitations with unperturbed frequency ω_T propagating in the forward and backward directions along z, and two purely photonic excitations with dispersion relation given by Eq. (9) that results from the Bragg scattering. If, on the other hand, the Bragg scattering is absent, i.e., $\Omega_B=0$, then the roots of Eq. (18) reduce to two pairs of polariton branches with the dispersion relation given by Eq. (15).

It appears that the unitary transformation in *four-dimensional* space diagonalizing the Hamiltonian $\mathcal{H}$ can be parametrized by *two* angles:

$$\begin{pmatrix} \hat{a}_{\rightarrow}(q) \\ \hat{a}_{\leftarrow}(-q) \\ \hat{b}_{\rightarrow}(q) \\ \hat{b}_{\leftarrow}(-q) \end{pmatrix} = \begin{pmatrix} \cos\theta\cos\tilde{\psi} & \sin\theta\sin\tilde{\psi} & \cos\theta\sin\tilde{\psi} & \sin\theta\cos\tilde{\psi} \\ \sin\theta\cos\tilde{\psi} & -\cos\theta\sin\tilde{\psi} & \sin\theta\sin\tilde{\psi} & -\cos\theta\cos\tilde{\psi} \\ \cos\theta\sin\tilde{\psi} & \sin\theta\cos\tilde{\psi} & -\cos\theta\cos\tilde{\psi} & -\sin\theta\sin\tilde{\psi} \\ \sin\theta\sin\tilde{\psi} & -\cos\theta\cos\tilde{\psi} & -\sin\theta\cos\tilde{\psi} & \cos\theta\sin\tilde{\psi} \end{pmatrix} \cdot \begin{pmatrix} \hat{\mathcal{B}}_2 \\ \hat{\mathfrak{I}}_2 \\ \hat{\mathfrak{I}}_1 \\ \hat{\mathcal{B}}_1 \end{pmatrix}, \tag{19}$$

where $\hat{\mathcal{B}}_1$, $\hat{\mathfrak{I}}_1$, $\hat{\mathfrak{I}}_2$, and $\hat{\mathcal{B}}_2$ are new operators that annihilate mixed light-matter states. The angle θ in Eq. (19) is precisely the ''Bragg'' rotation angle introduced in Eq. (7) [for simplicity we set $\phi=0$ for the modulation phase in Eq. (19)]. The second angle, $\tilde{\psi}$ is defined by the following relation:

$$\cos 2\tilde{\psi}=\frac{\sqrt{[\omega(q)-\omega(-q)]^2+4\Omega_B^2}-2(\omega_T-\omega_B)}{\sqrt{\{2(\omega_T-\omega_B)-\sqrt{[\omega(q)-\omega(-q)]^2+4\Omega_B^2}\}^2+16\Omega_P^2}}. \tag{20}$$

Naturally, for $\Omega_B=0$ the angle $\tilde{\psi}$ reduces to the polaritonic rotation angle ψ in Eq. (13). In the presence of the Bragg scattering, however, this rotation angle also depends on the ''Bragg'' parameters ω_B and Ω_B. Therefore it is the angle $\tilde{\psi}$ that characterizes the interplay between the polaritonic and diffraction effects.

IV. PCP EXCITATIONS

In order to analyze the solutions of Eq. (18), it is convenient to introduce the following dimensionless variables. We measure frequencies Δ from the Bragg frequency ω_B and express them in units of the Bragg gap $2\Omega_B$:

$$\Delta=\frac{\omega-\omega_B}{2\Omega_B}. \tag{21}$$

In analogy with Eq. (21), we introduce the dimensionless frequency detuning, δ, of ω_T from the Bragg frequency ω_B, where

$$\delta=\frac{\omega_T-\omega_B}{2\Omega_B}. \tag{22}$$

As seen from Eq. (9), the natural unit for the wave-vector deviation, q, from the Bragg wave vector, $\sigma/2$, is $\sigma\Omega_B/\omega_B$. Hence, we introduce the dimensionless parameter

$$Q=\left(\frac{\omega_B}{\sigma\Omega_B}\right)q. \tag{23}$$

With the new notations, the excitation spectrum determined by Eq. (18) can be rewritten in a more concise form

$$Q=\pm\sqrt{\left(\Delta-\frac{\alpha^2}{\Delta-\delta}\right)^2-\frac{1}{4}}, \tag{24}$$

where $\alpha=\Omega_P/(2\Omega_B)$ characterizes the relative strength of the Bragg and polaritonic couplings. Expression (24) is our main result. It clearly demonstrates that the Bragg and polaritonic dispersion relations *compete* with each other.

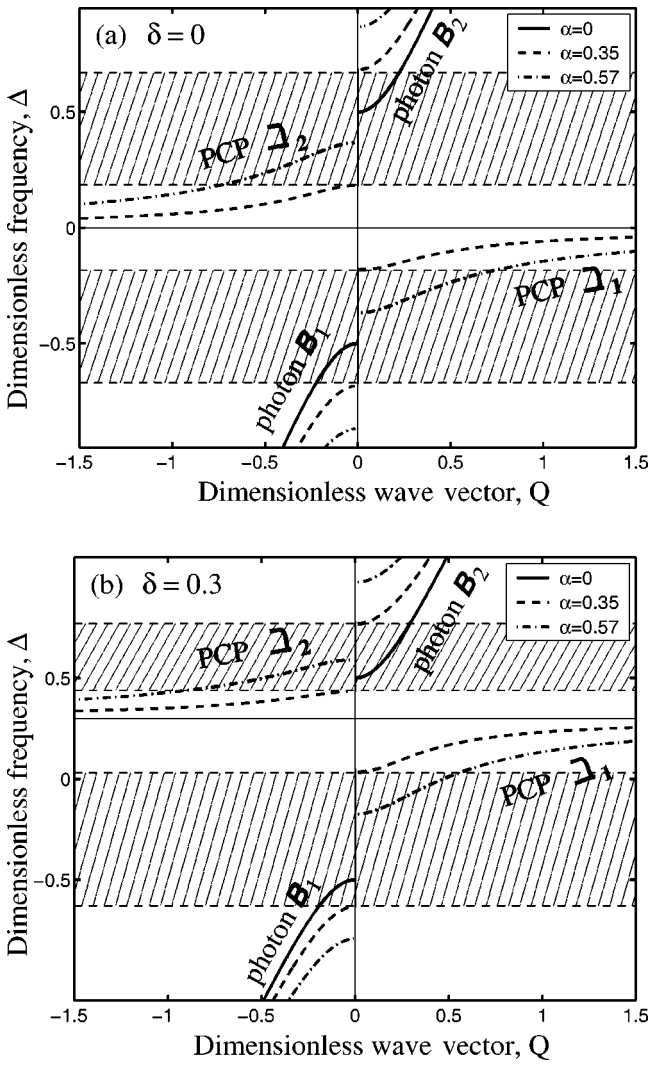

FIG. 1. Dispersion of mixed photonic-medium excitations for various coupling strengths: $\alpha=0,0.35,0.57$. (a) $\delta=0$; (b) $\delta=0.3$. The shaded area represents the two forbidden subgaps at $\alpha=0.35$.

Consider for simplicity the case of exact resonance, i.e., $\delta=0$. It is seen from Eq. (24) that in the absence of light-matter coupling ($\alpha=0$), the first term in the brackets gives rise to the conventional PBG. It is also seen that with increasing α (or, Ω_P), the decay length $\mathrm{Im}\,Q^{-1}$ increases, and for sufficiently small Δ we find that Q becomes *real*. This manifests the emergence of the *allowed* photonic states, or PCP excitations, inside the PBG (see Fig. 1). The PCP branches in the excitation dispersion relations are described by the operators $\hat{\mathfrak{I}}_1$ and $\hat{\mathfrak{I}}_2$. They occupy the frequency ranges $\Delta=[0,\pm\frac{1}{4}(\sqrt{1+16\alpha^2}-1)]$. For small α ($\alpha\ll 1$), the PCP frequency interval reduces to $(0,\pm 2\alpha^2)$. We note that due to the finite α value the Bragg gap broadens. Namely, the band edges of the branches described by the operators $\hat{\mathcal{B}}_1$, $\hat{\mathcal{B}}_2$ are, respectively, given for $\delta=0$ by $\Delta=\pm\frac{1}{4}(\sqrt{1+16\alpha^2}+1)$ (compare to $\Delta=\pm 1/2$ for $\alpha=0$). The dispersion relations $\Delta(Q)$ calculated using Eq. (24) are shown in Fig. 1(a) for different values of α in the case of exact resonance $\omega_B=\omega_T$, or $\delta=0$.

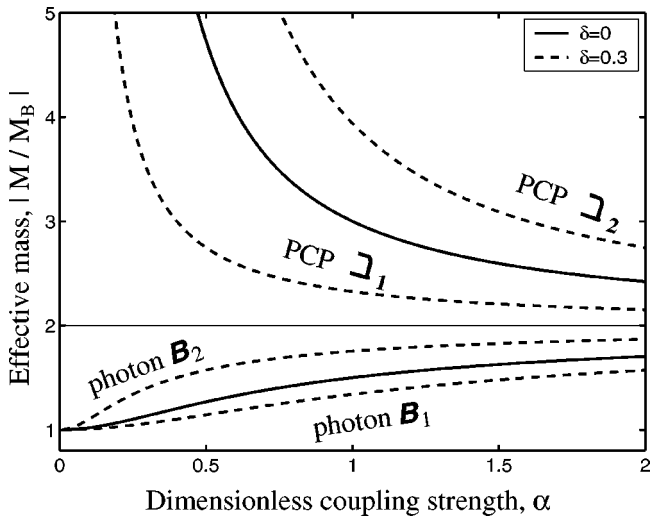

FIG. 2. The effective mass for various excitations (in units of ''free'' Bragg mass $M_{\mathcal{B}}=M_{\mathcal{B}_1}=M_{\mathcal{B}_2}$ at $\alpha=0$) is plotted vs coupling strength: solid lines are for $\delta=0$, where $M_{\mathcal{B}1}=M_{\mathcal{B}2}$, $M_{\mathfrak{I}_1}=M_{\mathfrak{I}_2}$; dashed lines are for $\delta=0.3$.

Moderate frequency detuning $\delta\neq 0$ does not qualitatively change the above picture as seen in Fig. 1(b). The major effect of frequency detuning is that the PCP branches $\mathfrak{I}_1$, $\mathfrak{I}_2$ acquire an asymmetry since they are ''pinned'' by ω_T. Figure 1 also shows that the Bragg-like photonic branches $\mathcal{B}_1$, $\mathcal{B}_2$ are affected by coupling or detuning only weakly.

To quantitatively describe the PCP dispersion relation, we consider two characteristics: (i) dimensionless effective mass M near the band edges that is defined from Eq. (24) by the relation

$$\Delta\simeq\Delta_{Q=0}+\frac{Q^2}{2M}, \tag{25}$$

and (ii) the density of states, $N(\Delta)$. Expanding Eq. (24) in Q yields the following effective masses for the PCP excitations:

$$M_{\mathfrak{I}_1}=\left[1-\frac{1-2\delta}{\sqrt{(1-2\delta)^2+16\alpha^2}}\right]^{-1}, \tag{26}$$

$$M_{\mathfrak{I}_2}=-\left[1-\frac{1+2\delta}{\sqrt{(1+2\delta)^2+16\alpha^2}}\right]^{-1}. \tag{27}$$

These masses are plotted in Fig. 2 versus the coupling strength α. For $\alpha\to 0$, we have $M_{\mathfrak{I}_1}$, $M_{\mathfrak{I}_2}\to\infty$, reflecting the fact that at $\alpha=0$ the PCPs reduce to dispersionless medium excitations that are not coupled to light. With the light-matter interaction switched on, the PCP effective mass rapidly decreases (the width of the in-gap branches increases).

The one-dimensional density of states $N(\Delta)$ is given from Eq. (24) by

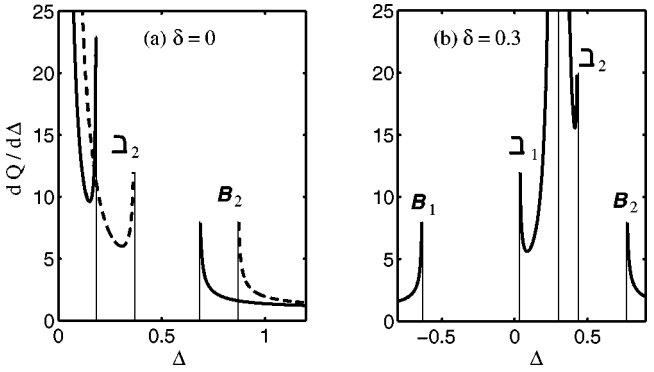

FIG. 3. Density of states for mixed photonic-medium excitations. Left panel is for the symmetric case ($\delta=0$), for $\alpha=0.35$ (solid line), and $\alpha=0.57$ (dashed line). Right panel is for $\delta=0.3$ and $\alpha=0.35$. The thin solid vertical lines indicate the band edges.

$$N(\Delta)\propto\frac{dQ}{d\Delta}=\frac{\Delta-\dfrac{\alpha^2}{\Delta-\delta}}{\sqrt{\left(\Delta-\dfrac{\alpha^2}{\Delta-\delta}\right)^2-\dfrac{1}{4}}}\left(1+\frac{\alpha^2}{(\Delta-\delta)^2}\right), \tag{28}$$

and shown in Fig. 3 for different values of α and detuning, δ. The density of states of the PCP branches inside the gap exhibits conventional 1D square-root singularities at the band edges $\Delta=\delta$ and $\Delta=\frac{1}{2}[\,\delta\mp\frac{1}{2}\pm\sqrt{(\delta\pm\frac{1}{2})^2+4\alpha^2}\,]$.

As mentioned above, the upper and lower Bragg-like photonic branches $\mathcal{B}_1$, $\mathcal{B}_2$ are only slightly affected by the coupling and/or detuning. In particular, their effective masses

$$M_{\mathcal{B}_1}=-\left[1+\frac{1+2\delta}{\sqrt{(1+2\delta)^2+16\alpha^2}}\right]^{-1}, \tag{29}$$

$$M_{\mathcal{B}_2}=\left[1+\frac{1-2\delta}{\sqrt{(1-2\delta)^2+16\alpha^2}}\right]^{-1}, \tag{30}$$

change only by a factor of 2 as α varies from zero to infinity (see Fig. 2).

V. INTRAGAP LOCALIZED STATES

We now turn our attention to the localized photonic states caused by a phase-slip-like defect. Note that in the absence of the polarizable medium, a structure with one-dimensional modulation (3) of the dielectric function can be viewed as a distributed feedback resonator [1] first considered by Kogelnik and Shank [23] in 1972. Later it was realized that a phase slip [24] in the modulation

$$\varepsilon(z)=\varepsilon_0+\delta\varepsilon\cos[\sigma z+\phi(z)], \tag{31}$$

where

$$\phi(z)=\begin{cases}\phi_1, & z<0,\\ \phi_2, & z>0\end{cases} \tag{32}$$

results in a localized state inside the PBG. Within the second quantization formalism of Sec. II, the emergence of such a state can be established as follows. Consider the eigenstate annihilation operators of the Hamiltonian (4),

$$\begin{pmatrix}\hat\beta_1\\ \hat\beta_2\end{pmatrix}=\begin{pmatrix}\cos\theta & -\sin\theta e^{i\phi}\\ \sin\theta e^{-i\phi} & \cos\theta\end{pmatrix}\begin{pmatrix}\hat a_{\rightarrow}\\ \hat a_{\leftarrow}\end{pmatrix}. \tag{33}$$

It follows from Eq. (33) that the absolute value λ of the amplitude ratio of the left and right propagating waves constituting the eigenstates β_1, β_2 is either $\lambda=\tan\theta$, or $\lambda=\tan^{-1}\theta$. These expressions are actually equivalent to the appropriate choice of the sign of square root:

$$\lambda_{\pm}(\Delta)=2\left(\Delta\pm\sqrt{\Delta^2-\frac{1}{4}}\right), \tag{34}$$

where we used the definition (7) of the rotation angle θ.

In the presence of a phase slip (32), the continuity condition at $z=0$ reads

$$\lambda_{-}(\Delta)e^{-i\phi_2}=\lambda_{-}^{*}(\Delta)e^{-i\phi_1}. \tag{35}$$

As is well known [25], Eq. (35) has a unique in-gap solution, Δ', for an arbitrary phase discontinuity $\phi_1-\phi_2$,

$$\Delta'=\cos\chi, \tag{36}$$

where

$$\chi=\begin{cases}\dfrac{\phi_1-\phi_2}{2}+\pi, & -\pi<\phi_1-\phi_2<0,\\ \dfrac{\phi_1-\phi_2}{2}, & 0<\phi_1-\phi_2<\pi.\end{cases} \tag{37}$$

Generalization of the above consideration to include the polarizable medium is straightforward. It reduces to the following modification of the parameter λ in Eq. (35):

$$\lambda_{\pm}(\Delta,\alpha,\delta)=2\left(\Delta-\frac{\alpha^2}{\Delta-\delta}\pm\sqrt{\left(\Delta-\frac{\alpha^2}{\Delta-\delta}\right)^2-\frac{1}{4}}\right). \tag{38}$$

Then condition (35) yields the gap state solution Δ',

$$\Delta'=\frac{1}{2}\left[\delta+\frac{1}{2}\cos\chi\pm\sqrt{\left(\delta-\frac{1}{2}\cos\chi\right)^2+4\alpha^2}\right], \tag{39}$$

where χ is defined by Eq. (37). For $\alpha=0$ we return to the in-gap state (36). Remarkably, we note that for nonzero coupling parameter α, when the Bragg gap is divided into two subgaps as in Fig. 1, the two values of Δ' determined by Eq. (39) are located in *each* of the corresponding subgaps. In Fig. 4 the frequencies Δ' of the localized in-gap states are shown versus the magnitude $\phi_1-\phi_2$ of the phase slip for zero detuning $\delta=0$.

In the case of opal photonic crystals, the phase slip considered above models a stacking fault. In fact, stacking faults are the most common defects in these structures [26].

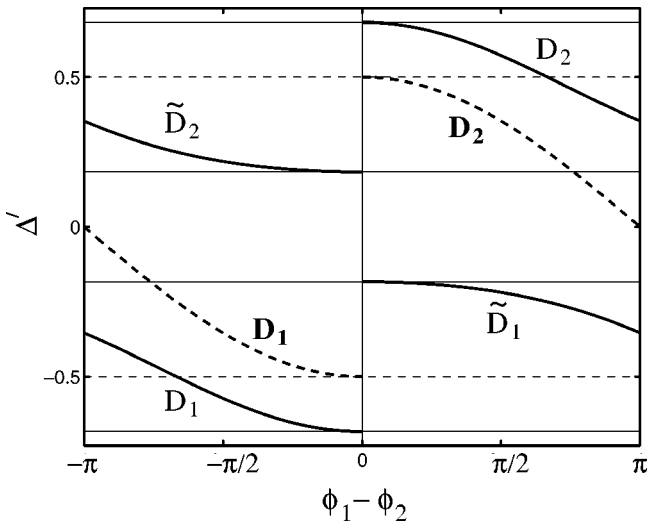

FIG. 4. The frequencies of localized intragap states vs the phase-slip magnitude: $\boldsymbol{D_1}$, $\boldsymbol{D_2}$ are defect levels inside the Bragg gap ($\alpha=0$, dashed line); D_1, $\tilde{D}_1$ are defect levels inside the lower subgap, and D_2, $\tilde{D}_2$ are defect levels inside the upper subgap ($\delta=0$, $\alpha=0.35$, solid line). Thin solid and dashed lines represent the band edges of the two forbidden gaps and of conventional Bragg gap (in the absence of coupling), respectively.

VI. DISCUSSION

The band structure of a photonic crystal with frequency-dependent dielectric function was recently studied numerically in Ref. [27], using the plane-wave method. In this work the photonic crystal was modeled as a two-dimensional array of GaAs rods. Frequency dispersion was introduced through the transverse-longitudinal splitting of the optical phonons. The authors [27] (see also Ref. [28]) observed that numerous branches of the band structure calculated for $\omega_B \equiv \omega_T$ become almost dispersionless at frequencies close to the frequency ω_T. One-dimensional realization of the situation [27] was considered in Ref. [29] and exhibited similar behavior.

In the context of the present work, this weakening of dispersion can be understood from Eqs. (26) and (26) that describe the effective masses of the PCP branches $\mathfrak{I}_1$, $\mathfrak{I}_2$. These masses rapidly increase as the coupling parameter α decreases. A more detailed comparison is impossible, since in order to show numerous dispersion curves, the authors of Refs. [27–29] choose a wide frequency scale that does not allow for identification of PCP branches.

It is important that our results are applicable for an oblique incidence at the arbitrary angle β. Indeed, in a photonic crystal with incomplete band gap, the general Bragg resonance condition is $\tilde{k}_z=\sigma/2$, where $\tilde{k}_z$ is the component of the wave vector $\tilde{\boldsymbol{k}}$ inside the photonic crystal along the modulation direction z [Eq. (3)]. If the interface is perpendicular to the modulation direction (e.g., parallel to the [111] plane of opal, which is the case in many experiments), then the wave-vector component parallel to the interface, $k \sin\beta$, is fixed by boundary conditions. In this case, the Hamiltonians, Eq. (4) and Eq. (16), correctly describe propagation along the z direction if $q=\tilde{k}_z-\sigma/2$ and the Bragg frequency and coupling are appropriately modified as $\omega_B(\beta)=\sigma c[2\sqrt{\varepsilon_0-\sin^2\beta}]^{-1}$, and $\Omega_B(\beta)=\omega_B(\beta)\delta\varepsilon[2(\varepsilon_0-\sin^2\beta)]^{-1}$. Correspondingly, all the results of this paper remain valid at the arbitrary incident angle if $\omega_B(\beta)$ and $\Omega_B(\beta)$ are used in the definitions of dimensionless parameters.

This opens an opportunity for experimental verification of the results. It was shown [26] that the absorption coefficient in self-assembled opal photonic crystals is as small as 1 cm^{-1}. The only region of strong absorption is in the close vicinity of medium resonance frequency ω_T. However, the width of this region is of the order of $\omega_{LT} \ll \Omega_P, \Omega_B$. Thus the existence of the propagating in-gap exitations and two forbidden gaps can be directly observed in measurements of transmission or reflection. The prime experimental manifestation of the PCP excitations derived in the present paper can be summarized as follows. Away from the resonance $\omega_B=\omega_T$, the polaritonic peak in the reflectivity spectrum occurs at $\omega=\omega_T$ regardless of the incident angle β. However, the variation of the Bragg peak frequency ω_B with β may lead to the resonance condition $\omega_B(\beta)\approx\omega_T$. At these angles *Bragg-diffracted* photons couple to the medium excitations resulting in the formation of the PCP branches. We predict that instead of a single Bragg reflection peak at the resonant condition, *two* reflection peaks may be observed that correspond to the two subgaps in the excitation spectrum. The frequencies of the *two* reflection bands become sensitive to the incident angle β, so that the angle-dependent reflectivity spectra will look as if the *polaritonic* peak *blueshifts* with increasing β. Note also that at exact resonance, namely when $\omega_B(\beta)=\omega_T$, the two reflection peaks would be the mirror images of each other.

Signatures of the behavior described above can be found in the numerical calculations of Ref. [30]. In that work, transmission spectra of a photonic crystal identical to that of Ref. [27] were calculated within the transfer-matrix formalism. *Two* minima in the transmission spectra were found instead of the usual *single* minimum that is caused by the Bragg diffraction in nondispersive photonic crystal. In light of the theory developed in the present work, these two minima can be identified with the *two forbidden subgaps* in the excitation spectrum (Figs. 1 and 3). As we have demonstrated (Fig. 3), in the presence of light-matter coupling there are two spectral regions with zero density of states. Correspondingly, the transmission coefficient within these frequency regions must be low if the sample is sufficiently thick.

A very different realization of periodic polarizable structures was the subject of extensive theoretical studies during the last decade [31,32]. The structures are multiple quantum wells separated by wide-gap semiconductor barriers. The width d of each barrier was assumed to be close to $\lambda_0/2$, where λ_0 is the wavelength corresponding to the intrawell exciton resonance frequency ω_T. The condition $d\approx\lambda_0/2$ implies that the Bragg frequency ω_B is close to ω_T. Since the quantum wells with strong frequency dispersion at $\omega\sim\omega_T$ had thickness much smaller than d, then a real Bragg gap in the structures [31,32] was lacking. However, under the condition $\omega_T \equiv \omega_B$, the dispersion law of light propagating along

the principal axis was shown to have a gap within a frequency range $|\omega-\omega_T|=(2\Gamma_0\omega_T/\pi)^{1/2}=\Omega^{(\mathrm{eff})}$. Here Γ_0 denotes the radiative rate for an exciton in a single well. In other words, $\Omega^{(\mathrm{eff})}$ plays the role of the ''effective'' Bragg gap in the structures [31,32]. Remarkably, a physical picture completely analogous to the multiple-quantum-well structures emerged from consideration of an optical lattice formed by laser-cooled atoms [33]. Correspondingly, the light dispersion relation derived in Ref. [33] has the same form as in Refs. [31,32]. Note that as was recently pointed out [34], a detuning $(\omega_B-\omega_T)\sim\Omega^{(\mathrm{eff})}$ gives rise to a band of propagating states within the ''effective'' Bragg gap of the multiple-quantum-well structures.

Yet another realization of a system combining Bragg and polaritonic properties was studied in Ref. [35]. Similarly to Refs. [31,32,34], the polarizable medium in Ref. [35] was restricted to a system of δ layers. In contrast to multiple quantum wells, the dispersive layers were immersed into the Bragg lattice. The presence of the two lattices in Ref. [35] makes the dispersion relation sensitive to their relative phase. Naturally, the excitation spectrum [35] is very different from Eq. (24). In particular, the authors of [35] observe only a single propagating in-gap excitation branch positioned asymmetrically with respect to the Bragg frequency.

ACKNOWLEDGMENTS

This work was supported by NSF Grant No. DMR 9732820, the Petroleum Research Fund under Grant No. ACS-PRF 34302-AC6, and the Army Research Office Grant No. DAAD 19-0010406.

[1] E. Yablonovitch, Phys. Rev. Lett. **58**, 2059 (1987).
[2] S. John, Phys. Rev. Lett. **58**, 2486 (1987).
[3] *Photonic Band Gaps and Localization*, edited by C. M. Soukoulis (Plenum, New York, 1993).
[4] J. D. Joannopoulos, R. D. Meade, and J. N. Winn, *Photonic Crystals: Molding the Flow of Light* (Princeton University Press, Princeton, NJ, 1995).
[5] S. L. McCall, P. M. Platzman, R. Dalichaouch, D. Smith, and S. Schultz, Phys. Rev. Lett. **67**, 2017 (1991).
[6] M. Plihal, A. Shambrook, A. A. Maradudin, and P. Sheng, Opt. Commun. **80**, 199 (1991).
[7] K. M. Ho, C. T. Chan, and C. M. Soukoulis, Phys. Rev. Lett. **65**, 3152 (1990).
[8] K. M. Leung and Y. F. Liu, Phys. Rev. Lett. **65**, 2646 (1990); Z. Zhang and S. Sapathy, *ibid.* **65**, 2650 (1990).
[9] S. John and J. Wang, Phys. Rev. B **43**, 12 772 (1991).
[10] S. John and T. Quang, Phys. Rev. A **50**, 1764 (1994).
[11] S. John and J. Wang, Phys. Rev. Lett. **64**, 2418 (1990).
[12] Z. Cheng and G. Kurizki, Phys. Rev. A **54**, 3576 (1996).
[13] W. Chen and D. L. Mills, Phys. Rev. Lett. **58**, 160 (1987); D. L. Mills and S. E. Trullinger, Phys. Rev. B **36**, 947 (1987); S. John and N. Aközbek, Phys. Rev. Lett. **71**, 1168 (1993); A. Kozhekin and G. Kurizki, *ibid.* **74**, 5020 (1995).
[14] S. John and T. Quang, Phys. Rev. Lett. **74**, 3419 (1995); **76**, 1320 (1996).
[15] A. Z. Genack, Phys. Rev. Lett. **58**, 2043 (1987).
[16] R. D. Meade, K. D. Brommer, A. M. Rappe, and J. D. Joannopoulos, Phys. Rev. B **44**, 13 772 (1991).
[17] O. Painter, R. K. Lee, A. Scherer, A. Yariv, J. D. O'Brien, P. D. Dapkus, I. Kim, Science **284**, 1819 (1999).
[18] C. Kittel, *Quantum Theory of Solids* (Wiley, New York, 1963).
[19] V. I. Rupasov and M. Singh, Phys. Rev. Lett. **77**, 338 (1996); Phys. Rev. A **54**, 3614 (1996); **56**, 898 (1997).
[20] S. John and V. I. Rupasov, Phys. Rev. Lett. **79**, 821 (1997); Europhys. Lett. **46**, 326 (1999).
[21] A. A. Zakhidov, R. H. Baughman, Z. Iqbal, C. Cui, I. Khayrullin, S. O. Dantas, J. Marti, and V. G. Ralchenko, Science **282**, 897 (1998).
[22] V. B. Berestetskii, E. M. Lifshitz, and L. P. Pitaevskii, *Quantum Electrodynamics* (Pergamon, Oxford, 1982).
[23] H. Kogelnik and C. V. Shank, J. Appl. Phys. **43**, 2328 (1972).
[24] S. L. McCall and P. M. Platzman, IEEE J. Quantum Electron. **QE-21**, 1899 (1985).
[25] E. A. Avrutin and M. E. Raikh, Sov. Phys. Tech. Phys. **33**, 1170 (1989).
[26] Yu. A. Vlasov, M. A. Kaliteevski, and V. V. Nikolaev, Phys. Rev. B **60**, 1555 (1999).
[27] V. Kuzmiak, A. A. Maradudin, and A. R. McGurn, Phys. Rev. B **55**, 4298 (1997).
[28] W. Zang, A. Hu, X. Lei, N. Xu, and N. Ming, Phys. Rev. B **54**, 10 280 (1996).
[29] A. Maradudin, V. Kuzmiak, and A. R. McGurn, in *Photonic Band Gap Materials*, Vol. 315 of *NATO ASI Series E: Applied Sciences*, edited by C. M. Soukoulis (Kluwer Academic, Dordrecht, 1996), p. 271.
[30] M. M. Sigalas, C. M. Soukoulis, C. T. Chan, and K. M. Ho, Phys. Rev. B **49**, 11 080 (1994).
[31] E. L. Ivchenko, Sov. Phys. Solid State **33**, 1344 (1991); for review see E. L. Ivchenko and M. Willander, Phys. Status Solidi B **215**, 199 (1999), and references therein.
[32] L. C. Andreani, Phys. Lett. A **192**, 99 (1994).
[33] I. H. Deutsch, R. J. C. Spreeuw, S. L. Rolston, and W. D. Phillips, Phys. Rev. A **52**, 1394 (1995).
[34] L. I. Deych and A. A. Lisyansky, Phys. Rev. B **62**, 4242 (2000).
[35] A. E. Kozhekin, G. Kurizki, and B. A. Malomed, Phys. Rev. Lett. **81**, 3647 (1998); T. Opatrný, B. A. Malomed, and G. Kurizki, Phys. Rev. E **60**, 6137 (1999).